

Stability analysis and treatment of a reservoir landslide under impounding conditions: a case study

Qinghui Jiang^{1,2} · Wei Wei² · Ni Xie² · Chuangbing Zhou^{1,2}

Received: 29 December 2014 / Accepted: 7 July 2015 / Published online: 16 December 2015
© Springer-Verlag Berlin Heidelberg 2015

Abstract The Muchanghe landslide is located on the left bank of the Muchang River in Dongping reservoir, Hubei Province, China. During reservoir impoundment, cracking and dislocation deformations occurred at the front and middle parts of the Muchanghe landslide. Once the landslide was triggered, the river could be blocked, which would lead to a serious threat to upstream flood control safety. In this study, the engineering geological properties and deformation characteristics of the Muchanghe landslide during impoundment were analyzed. A 3-D limit equilibrium method was proposed for the stability analysis of this asymmetric landslide. Based on the proposed 3-D method, a visualization program (JSlope3D) was developed and applied to evaluate the stability of the Muchanghe landslide. The results indicated that the stability of the landslide gradually decreases with the rise of impounding water level in the Dongping reservoir. When the impounding water level reaches an elevation of 490 m (normal pool level), the calculated factor of safety predicted that the landslide would be in an unstable state. To prevent the generation of a landslide failure, a reinforcement scheme involving the cutting back of the slope and backfill was proposed to improve the stability of the landslide. Using the proposed 3-D method, the Muchanghe landslide, after stabilization, was stable at different impoundment water levels and can satisfy the requirements of the design specification.

Keywords Muchanghe landslide · Reservoir impounding · Three-dimensional limit equilibrium method · Factor of safety · Cutting slope and backfill

Introduction

The construction of a reservoir brings human benefits such as navigation, irrigation, and electricity generation, but it also generates geohazards such as landslides. Once landslides occur within the reservoir area, they can not only destroy hydraulic structures directly, but also cause reservoir sedimentation and thus decrease the effective storage volume thereof. Moreover, the sliding mass slips into the reservoir at a high speed, which would cause a surge and threaten the safety of both the dam and people. For instance, on October 9, 1963, the Vaiont reservoir disaster happened on the Piave River, Italy. In this case, a sliding mass with an area of $1.8 \text{ km} \times 1.6 \text{ km}$ slipped down the hillside, at high speed, and created a huge wave, which overtopped the dam by 100 m and swept down the valley, causing 2600 fatalities (Kiersch 1964). In China, a serious incident resulting from impoundment took place at Zhexi Reservoir in Hunan Province (Jin and Wang 1988). The volume of the sliding mass was about $165 \times 10^4 \text{ m}^3$, which slipped into the reservoir at a speed of 19.53 m/s. The surge caused by this landslide flowed over the dam, which was still under construction, discharged downstream, flooded the construction pit, and killed over 40 people. To reduce this kind of loss, reservoir impounding-induced landslide hazard assessment is important and helpful to landslide prevention and mitigation in the ongoing construction of hydropower stations and after reservoir filling.

Although some sophisticated numerical methods, such as the finite element method (Ugai 1989; Zheng et al. 2005;

✉ Qinghui Jiang
jqh1972@whu.edu.cn

¹ School of Civil Engineering and Architecture, Nanchang University, Nanchang 330031, People's Republic of China

² School of Civil Engineering, Wuhan University, Wuhan 430072, People's Republic of China

Griffiths and Marquez 2007), discrete element method (Corkum and Martin 2004; Lee and Hencher 2013), and discontinuous deformation analysis method (Jiang et al. 2013; Xu et al. 2014), have been applied to the stability assessment and failure prediction of landslides, conventional limit equilibrium methods are still playing a major role in practice. Usually, landslide stability was analyzed by limit equilibrium methods in two dimensions. The 2D analyses simplify the problem into plane strain conditions and cannot properly model the true three-dimensional characteristics of landslides. As pointed out by Stark and Eid (1998), 3-D analyses are beneficial for stability assessment and stabilization treatment of landslides with complicated failure surfaces. Recently, a number of 3-D limit equilibrium methods for landslide stability analysis have been presented based on extensions of corresponding 2-D methods (Chen and Chameau 1982; Baker and Leshchinsky 1987; Zhang 1988; Hungr et al. 1989; Leshchinsky and Huang 1992; Lam and Fredlund 1993; Chen et al. 2001; Zheng 2012; Sun et al. 2012; Zhou and Cheng 2013). Since a plane of symmetry, or direction of sliding, is implicitly assumed in the analysis, these 3-D methods are only appropriate for landslides with a symmetric geometry. Yamagami and Jiang (1997), Huang et al. (2002), and Cheng and Yip (2007) further developed 3-D limit equilibrium methods for asymmetric slopes and landslides. Due to their involving complex and time-consuming iterative procedures for determining the unknowns, the aforementioned methods are still of limited use for practical problems.

The Dongping Hydropower Station is located in the downstream reaches of the Zhongjian River in Xuan'en County, Hubei Province, China (Fan et al. 2007). It is a hydroelectric project which combines shipping, transportation, flood protection, and aquaculture. The normal pool level of the reservoir is 490 m, and the total storage capacity reaches $3.43 \times 10^8 \text{ m}^3$. The construction of the Dongping Hydropower Station started in March 2002. It began to impound in March 2005 and reached a water level of about 470 m in September 2006. Due to the effects of reservoir impoundment, deformation, fissuring, and dislocations emerged on the Muchanghe landslide mass. The maximum width of the fissures reached 0.5 m with a fall of 0.4 m between both walls. Although there were no residents living on the landslide mass, the width of river here is relatively narrow. Once the landslide was triggered, it might block the river and threaten the safety of Xuan'en County located upstream. Therefore, it was necessary to estimate the stability of the Muchanghe landslide and determine appropriate stabilization measures. The deformation characteristics of the Muchanghe landslide, after reservoir impounding, were investigated. Given that the Muchanghe landslide has a complicated geometry and

pore-water pressure conditions, a 3-D asymmetric landslide stability method was proposed to evaluate the influence of reservoir impoundment on the stability of the landslide. The corresponding reinforcement measures were also provided. The research results can provide a reference for the stability assessment and reinforcement design of similar landslides in reservoir areas.

Description of the Muchanghe landslide

The Muchanghe landslide is located on the left bank of Dongping reservoir. It is about 20 km from the downstream dam and 10 km from Xuan'en County which lies upstream. This section of the Muchang River runs on an L-shaped bend. The geological map of the Muchanghe landslide area is shown in Fig. 1. The elevations of its leading edge and trailing edge are 450–452 and 640–650 m, respectively. The sliding mass covers a semi-oval area of about $6.42 \times 10^4 \text{ m}^2$, and its total volume is about $310 \times 10^4 \text{ m}^3$. The topography of the landslide mass is stepped, with slope angles between 35° and 45° and a relatively gentle section in the middle part. The elevation of the mountain lies between 800 and 900 m at its peak. The upper part of the mountain in the area of the landslide is massive, and its lower part is deeply incised by the river valley. The strike of the mountain ridge is basically identical with the direction of water flow, and the slope body is cut into fan-shaped steps by gullies.

Exploratory drilling reveals that the sliding surface mainly consists of the contact interface between bed rock and the Quaternary system (Fig. 2). The material composition of the sliding band is isabelline clay with gravels. The thickness of the sliding band is about 0.4 m. With regard to the sliding mass, it consists of diluvial and colluvial deposits of the Holocene series of Quaternary system. It is mainly composed of gravelly soil, mild clay (with gravels), and stones. The bed rock beneath the sliding mass consists of a Lower Triassic laminated limestone of the Daye Group. The dips of the strata are relatively gentle and are between 15° and 20° : Together they form a dip slope. The bed rock, i.e., the limestone, is weakly weathered, and fissures in the bed rock are developed with a high permeability to water.

Deformation characteristics after reservoir impounding

The Dongping Hydropower Station started to impound in March 2005 and reached a water level of about 470 m in September 2006. It reached its maximum water level of 482 m in August 2007. Due to reservoir impoundment, the

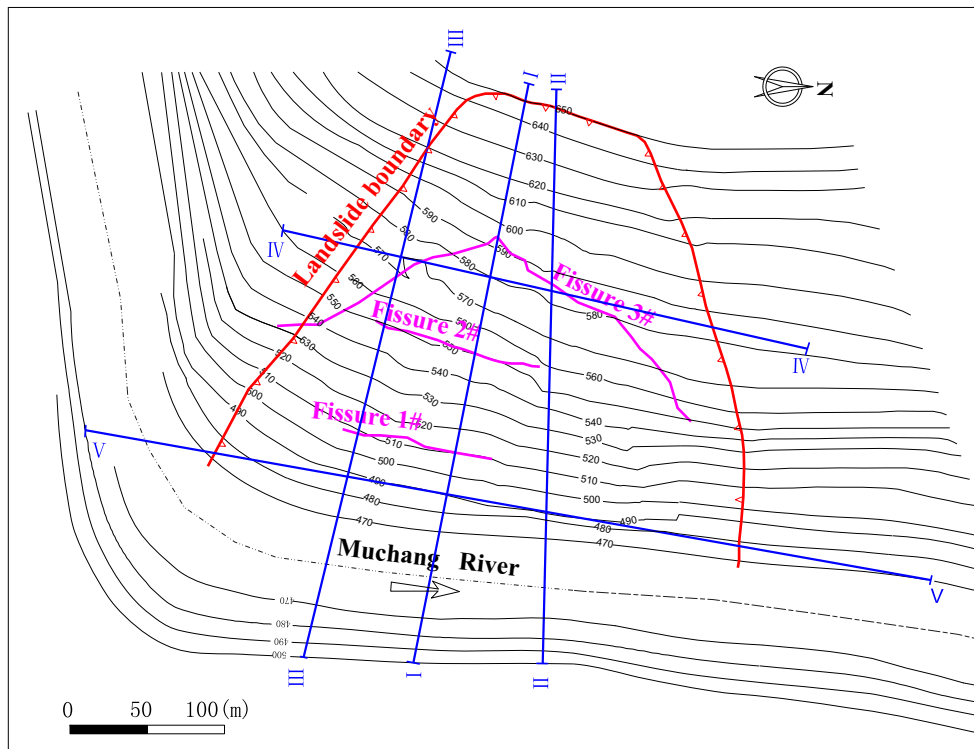
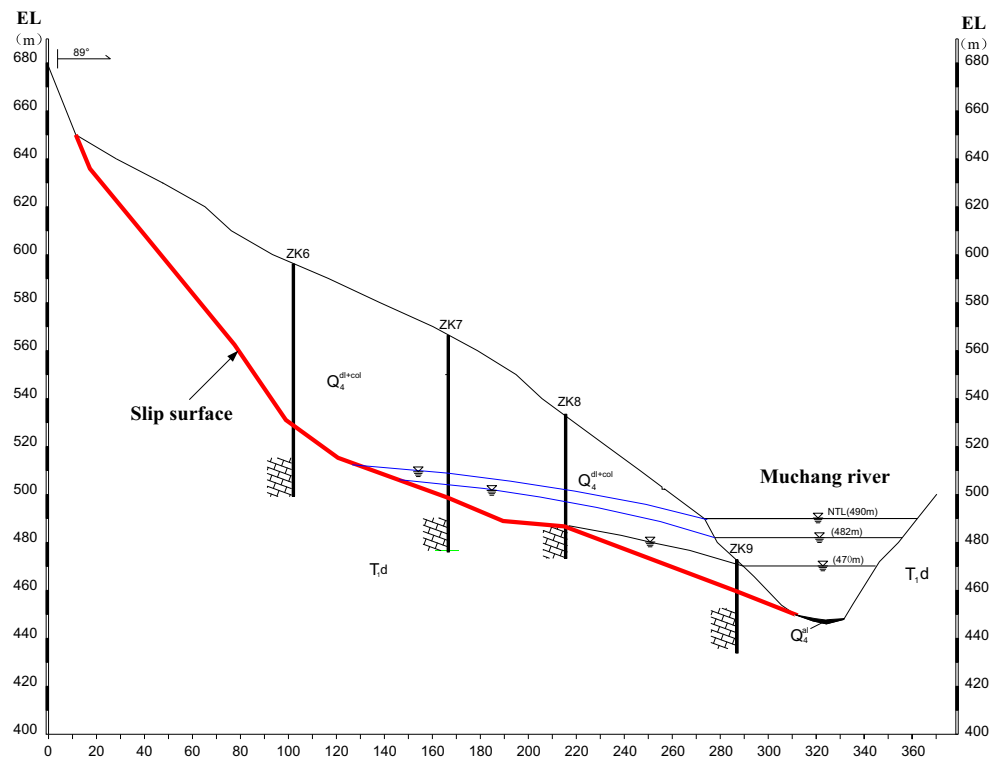


Fig. 1 Geological plan view of the Muchanghe landslide

Fig. 2 The II–II geological profile of the Muchanghe landslide



surface layer of soil in the Muchanghe landslide began to deform significantly. In September 2006, two transverse fissures (fissure 1# and fissure 2#) developed at the front

and middle parts of the landslide mass (see Fig. 1), which strike in an SN direction, trending E, with a dip angle of 70°–80°. The fissures are about 80–150 m long and

0.15–0.40 m wide. Stairs were formed with a fall of about 0.1–0.3 m. In August 2007, it is found that the original fissures, fissure 1# and fissure 2#, further extended in length and expanded in width. A new fissure, fissure 3#, emerged at an elevation of between 550 and 595 m. It was arc-shaped in the horizontal plane, with a length of over 200 m and a width of about 0.4 m. The fall between the two fissure walls was about 0.3 m, and its visible depth was about 0.3 m. This fissure had a tendency, and the potential, to grow.

From the locations of fissures 1#, 2#, and 3#, and their order of appearance, together with the deformation characteristics of the landslide mass, it can be revealed that the stability of the Muchanghe landslide is closely related to the reservoir impoundment and it exhibits the features of a trail-type landslide. Since the sliding mass of the Muchanghe landslide is mainly composed of gravelly soil and silty clay, its mechanical properties are weak with a high void ratio, a high permeability, and little apparent cohesion. After impoundment, the soaking and weakening effects of reservoir water lead to significant decreases of both the cohesion and friction angle of the soil at the front edge of the sliding mass. Thus, the shear strength of the front edge is significantly reduced. Meanwhile, the landslide mass is permeable and fractures are extensively developed throughout its central and lower parts. Thus, the reservoir impoundment causes seepage of groundwater within the landslide mass, which results in a rising groundwater level and the increased pore pressures. Additionally, because of the repeated scouring action of reservoir water, it is easy for the landslide mass to deform or suffer local collapses. Therefore, under the comprehensive effects of all these factors, the toe of the front edge deformed and cracked, and this then drove the whole landslide mass to slip. This type of landslide is a typical bedding landslide occurring along the contact interface between bed rock and Quaternary deposits.

Stability analysis

A three-dimensional limit equilibrium method

For 3-D stability analysis, the potential failure mass is divided into a number of columns with vertical interfaces. At the ultimate equilibrium state, the internal and external forces acting on each column are shown in Fig. 3. To make the problem statically determinate, the following assumptions are introduced in the present 3-D formulation:

1. All columns have the same sliding direction, denoted by β , on the plan view of the failure mass (see Fig. 4).

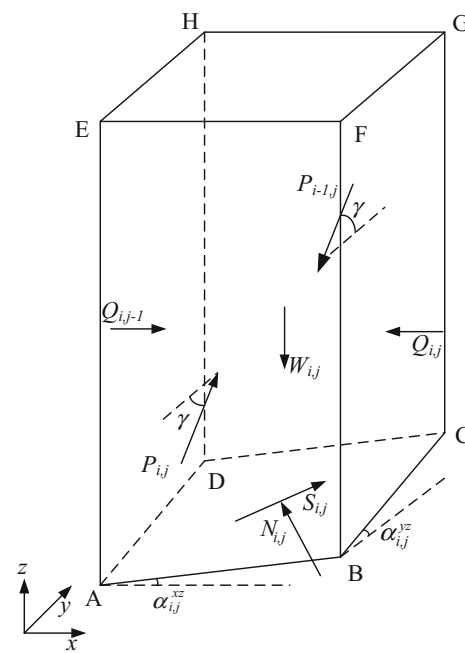


Fig. 3 Forces acting on a typical column (i, j)

2. The horizontal intercolumn shear forces are negligible. It is further assumed that the intercolumn force P on the row interfaces has the same inclination of γ to the y -axis throughout the whole failure mass (see Fig. 3). In addition, the vertical shear forces acting on the

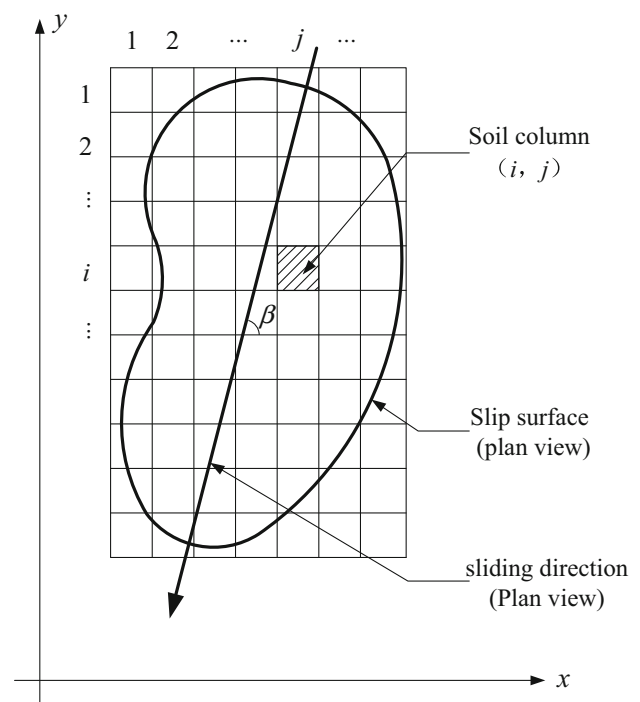


Fig. 4 Plan view of divided columns and slip surface

column interfaces are also neglected, i.e., only the normal force Q in the x -direction is applied to the column interfaces. Similar assumptions have been made by Chen et al. (2003).

By the Mohr–Coulomb criteria, the factor of safety, F , is defined as

$$F = \frac{\tan \phi' (N_{i,j} - U_{i,j}) + c' A_{i,j}}{S_{i,j}} \tag{1}$$

where $N_{i,j}$, $S_{i,j}$, and $U_{i,j}$ denote the total normal force, mobilized shear force, and pore-water force acting on the base of column (i, j) , respectively; ϕ' , c' , and A are the effective friction angle, effective cohesion, and the base area of the column, respectively.

According to assumption (1), the unit vectors \mathbf{n} and \mathbf{s} of the total normal force $N_{i,j}$ and mobilized shear force $S_{i,j}$ on the column base can be expressed as

$$\begin{aligned} \mathbf{n} &= [n_x \quad n_y \quad n_z]^T \\ &= [-\tan \alpha_{i,j}^{xz} / J \quad -\tan \alpha_{i,j}^{yz} / J \quad 1/J]^T \end{aligned} \tag{2}$$

$$\begin{aligned} \mathbf{s} &= [s_x \quad s_y \quad s_z]^T \\ &= [\cos \beta / J' \quad \sin \beta / J' \quad (\cos \beta \tan \alpha_{i,j}^{xz} + \sin \beta \tan \alpha_{i,j}^{yz}) / J']^T \end{aligned} \tag{3}$$

in which

$$J = \sqrt{1 + \tan^2 \alpha_{i,j}^{xz} + \tan^2 \alpha_{i,j}^{yz}} \tag{4}$$

$$J' = \sqrt{1 + (\tan \alpha_{i,j}^{xz} \cos \beta + \tan \alpha_{i,j}^{yz} \sin \beta)^2} \tag{5}$$

where $\alpha_{i,j}^{xz}$ and $\alpha_{i,j}^{yz}$ are the base inclination relative to the x - and y -axes at the center of each column, respectively, as defined in Fig. 3.

The force equilibrium equations for column (i, j) can be expressed as

$$\mathbf{n}N_{i,j} + \mathbf{s}S_{i,j} - \mathbf{k}W_{i,j} + \mathbf{p}(P_{i,j} - P_{i-1,j}) + \mathbf{i}(Q_{i,j-1} - Q_{i,j}) = 0 \tag{6}$$

where $W_{i,j}$ is the weight of the column and $\mathbf{k} = [0 \quad 0 \quad 1]^T$ denotes the unit vector in the positive z -axis direction; $\mathbf{p} = [0 \quad \cos \gamma \quad \sin \gamma]^T$ denotes the unit vector of the intercolumn force P ; and $\mathbf{i} = [1 \quad 0 \quad 0]^T$ denotes the unit vector in the positive x -axis direction.

With reference to Fig. 5, $\mathbf{p}' = [0 \quad -\sin \gamma \quad \cos \gamma]^T$ is defined as the unit vector perpendicular to the intercolumn force P . The total normal force acting on the column base can be derived from the force equilibrium condition in the direction of \mathbf{p}' . Based on the scalar product of Eq. (6) and \mathbf{p}' , it follows that

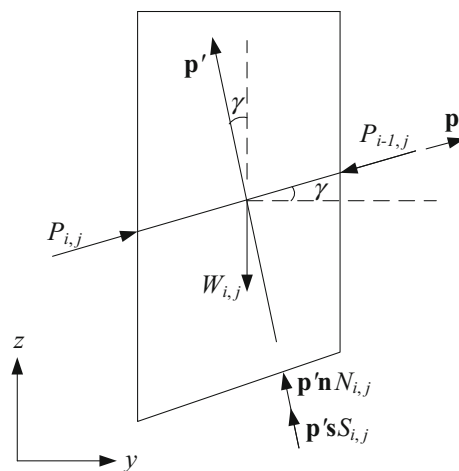


Fig. 5 Projection of forces acting the column on the y - z plane

$$N_{i,j}(n_z \cos \gamma - n_y \sin \gamma) + S_{i,j}(s_z \cos \gamma - s_y \sin \gamma) - W_{i,j} \cos \gamma = 0 \tag{7}$$

Substituting Eq. (1) into Eq. (7), we obtain

$$N_{i,j} = \frac{(c' A_{i,j} - U_{i,j} \tan \phi')(s_y \sin \gamma - s_z \cos \gamma) + F W_{i,j} \cos \gamma}{F(n_z \cos \gamma - n_y \sin \gamma) + (s_z \cos \gamma - s_y \sin \gamma) \tan \phi'} \tag{8}$$

By projecting the forces acting on the whole failure mass in the direction of \mathbf{p} , we obtain

$$\sum N_{i,j}(n_y \cos \gamma + n_z \sin \gamma) + \sum S_{i,j}(s_y \cos \gamma + s_z \sin \gamma) - \sum W_{i,j} \sin \gamma = 0 \tag{9}$$

Establishing the overall force equilibrium equation in the x -direction leads to

$$\sum N_{i,j}n_x + \sum S_{i,j}s_x = 0 \tag{10}$$

Establishing the overall moment equilibrium equation about the x -axis leads to

$$\sum N_{i,j}(n_z y_0 - n_y z_0) + \sum S_{i,j}(s_z y_0 - s_y z_0) - \sum W_{i,j} y_0 = 0 \tag{11}$$

where (x_0, y_0, z_0) are coordinate values of the center of the base of column (i, j) .

There are three unknowns, namely the factor of safety (F), the overall sliding direction (β), and the inclination (γ) of the intercolumn force involved in Eqs. (9), (10), and (11). Newton’s method is used to solve the three unknowns, and the initial values of the unknowns are set to be $F_0 = 1.0$, $\beta_0 = 1.0$, and $\gamma_0 = 0.0$ in the present study. Two typical examples that have been documented in the literature are selected to verify the effectiveness and

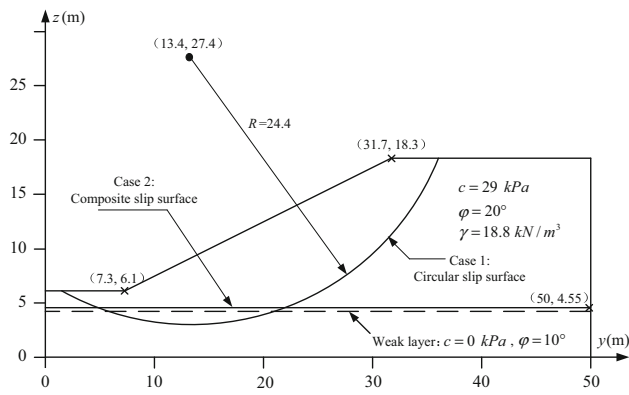


Fig. 6 Slope geometry for Example 1

Table 1 Results for two different cases in Example 1

	Factor of safety	Direction of sliding (Radian)	Inclination of intercolumn forces (Radian)	Iteration times
Case 1	2.132	1.57	0.254	8
Case 2	1.783	1.57	0.203	5

Total column number = 1852 (column size: 1 m × 1 m)

precision of the proposed method. Example 1 is taken from Zhang (1988), as illustrated in Fig. 6. The problem was analyzed for two different cases. Case 1 involves a failure surface which is circular in the y - z plane and ellipsoidal in the out-of-plane direction. In Case 2, the part of the ellipsoidal failure surface below $z = 4.55$ m is truncated by a weak layer. Using the proposed 3-D method, we obtained results for the two cases which are listed in Table 1. It is interesting to note that the solution for the sliding direction is 1.57 (in radians), as would be anticipated for the problem with the symmetric failure surfaces. The example has been used by various investigators to validate their 3D analysis methods. Zhang (1988) proposed a simplified 3-D version of Spencer’s method in which the inclination of the resultant of all intercolumn forces is assumed to be a constant. Hungr et al. (1989) developed their 3-D Bishop’s method by neglecting the vertical shear force components of the intercolumn force. Huang et al. (2002) presented a generalized 3-D method which is practically equivalent to Janbu’s rigorous method with some simplifications

Table 2 Comparison of the factors of safety from various methods

Method	Zhang (1988)	Hungr et al. (1989)	Huang et al. (2002)	Chen et al. (2003)	Zheng (2012)	Sun et al. (2012)	Present study
Case 1	2.122	2.167	2.215	2.187	–	2.000	2.132
Case 2	1.553	1.620	1.757	1.640	1.735/1.766	1.677–1.680	1.783

involving the transverse shear forces. Zheng (2012) and Sun et al. (2012) presented their non-column-based method in which normal stresses on the slip surface are modified by a function with five parameters. Table 2 gives the calculated factors of safety from these methods. It can be seen that for the problem with symmetric failure surfaces, the factors of safety obtained using different approaches are in reasonably close agreement.

Example 2 (see Fig. 7) is taken from Cheng and Yip (2007) and involves an asymmetric rigid block failure. The safety factor and sliding direction (rotating counterclockwise from the x -axis) can be determined explicitly as 0.280 and 2.035 (in radians). Using the proposed 3-D method, we have obtained a safety factor of 0.279 and a sliding direction of 2.034. The solutions for Examples 1 and 2 are correctly predicted by the proposed method, which demonstrates the validity of the proposed method for 3-D slope stability problems. In addition, the results from all the examples in this study indicate that Newton’s method converged rapidly.

Stability of the Muchanghe landslide

Based on the proposed 3-D limit equilibrium method, a visualization program, named JSlope3D, was developed for the stability analysis of landslides. The 3-D geological modeling of landslides is a key part of developing the visualization program because it provides both geometrical and geological information for limit equilibrium solutions. By fitting the geometric datum of the ground surface and sliding surface, we can establish a 3-D geological model of each landslide. As a user-friendly interface, and high-performance graphics capabilities, is important in any a visualization program, the view of JSlope3D consists of interactive 2-D and 3-D graphics, as shown in Fig. 8. The former mainly displays the plan view of the landslide and mesh used for subsequent analysis: The latter contains 3-D graphics displaying the landslide.

JSlope3D was used to evaluate the stability of the Muchanghe landslide both before and after reservoir impounding. The mechanical parameters given by the designer for the sliding mass and slip band are listed in Table 3. Based on a comprehensive compilation of shear

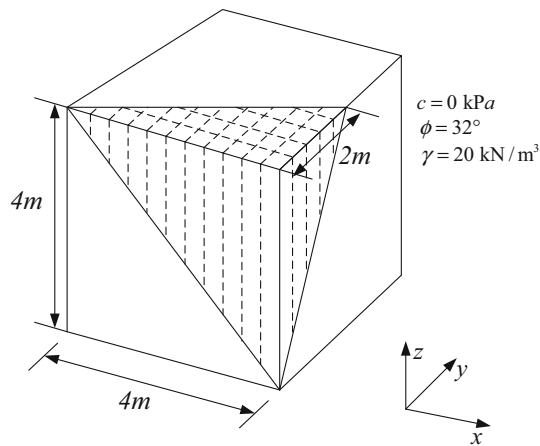


Fig. 7 Slope geometry for Example 2

test evidence, the judgments of several experienced geotechnical engineers and geologists in this region, the strength parameters for the sliding belt were given as: $c' = 25 \text{ kPa}$ and $\phi' = 27.5^\circ$. The underground water level in the landslide (see Fig. 2) is determined based on drilling observations of groundwater and seepage analysis during reservoir impounding (Hubei Provincial Water Resources and Hydropower Planning Survey and Design Institute 2007). The size of columns for discretization of the sliding mass was $5 \text{ m} \times 5 \text{ m}$. It is noted that calculations were carried out only for those columns within slide limits (see Fig. 8). The safety factors of the Muchanghe landslide, when subjected to different water levels, are listed in Table 4.

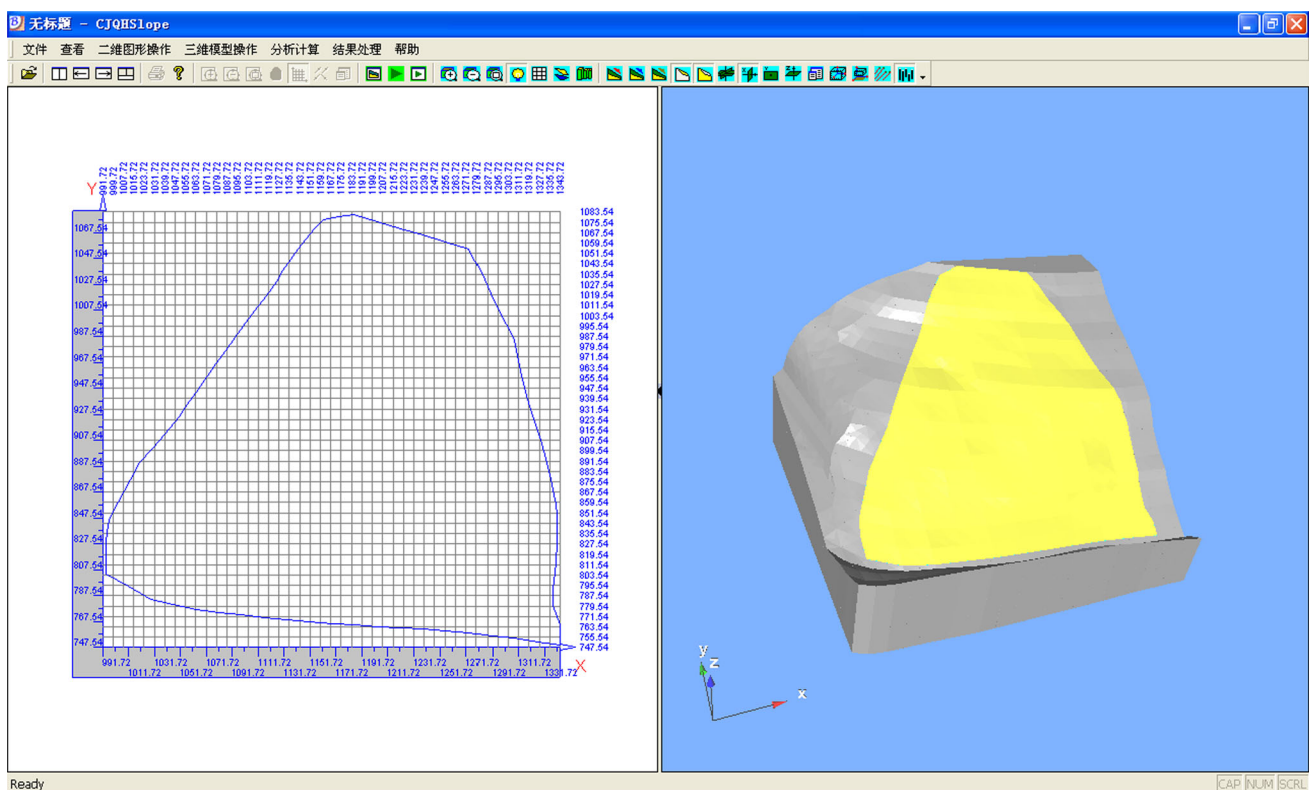


Fig. 8 3-D visualization model and the division mesh of the Muchanghe landslide

Table 3 Mechanical parameters of the Muchanghe landslide

	Unit weight (kN/m^3)		Friction angle	Cohesion (kPa)
	Natural	Saturated		
Sliding mass	19.5	21	–	–
Sliding band	–	–	27.5	25
Backfill body	19.5	21	–	–

Table 4 Factors of safety of the Muchanghe landslide

No.	Case	Original topography		After treatment	
		Factor of safety	Direction of sliding	Factor of safety	Direction of sliding
1	Before impounding	1.111	1.268	1.254	1.288
2	470 m of reservoir water level	1.064	1.267	1.181	1.287
3	482 m of reservoir water level	1.011	1.268	1.126	1.290
4	490 m of reservoir water level	0.984	1.268	1.101	1.292

The results given in Table 4 show that the safety factor of the Muchanghe landslide before impoundment was 1.111, which indicates that the Muchanghe landslide was stable before impoundment. As the reservoir water level was increased, the safety factor of the Muchanghe landslide gradually decreased, revealing that reservoir impoundment was an important external factor inducing landslide deformation. When the reservoir water rose to a level of 482 m, the safety factor of the Muchanghe landslide was 1.011, which demonstrated a critical state verging on instability. This result is consistent with the in situ observation of large deformations at the front edge and middle part of the landslide mass, accompanied by the generation of the transverse connected fissure (fissure 3#). When the reservoir was impounded to its normal pool level of 490 m, the safety factor of the Muchanghe landslide decreased to 0.984. Hence, combining with the deformation characteristics of the Muchanghe landslide

after impoundment and the results of 3-D stability analyses, it is predicted that the landslide mass is likely to lose its stability and slip in the direction N72.65°W. Once the failure of the landslide happens, it can impair the flood control safety of Xuan'en County (upstream). Therefore, stabilization treatment was necessary for the Muchanghe landslide.

Stabilization treatment

Stabilization methods

Given that the front edge of the Muchanghe landslide is fairly thick, if we select anti-slide piles as a stabilization measure, both the amount of work and its cost will be huge. However, if we choose stabilization methods involving both cutting back of slope and backfilling, the required

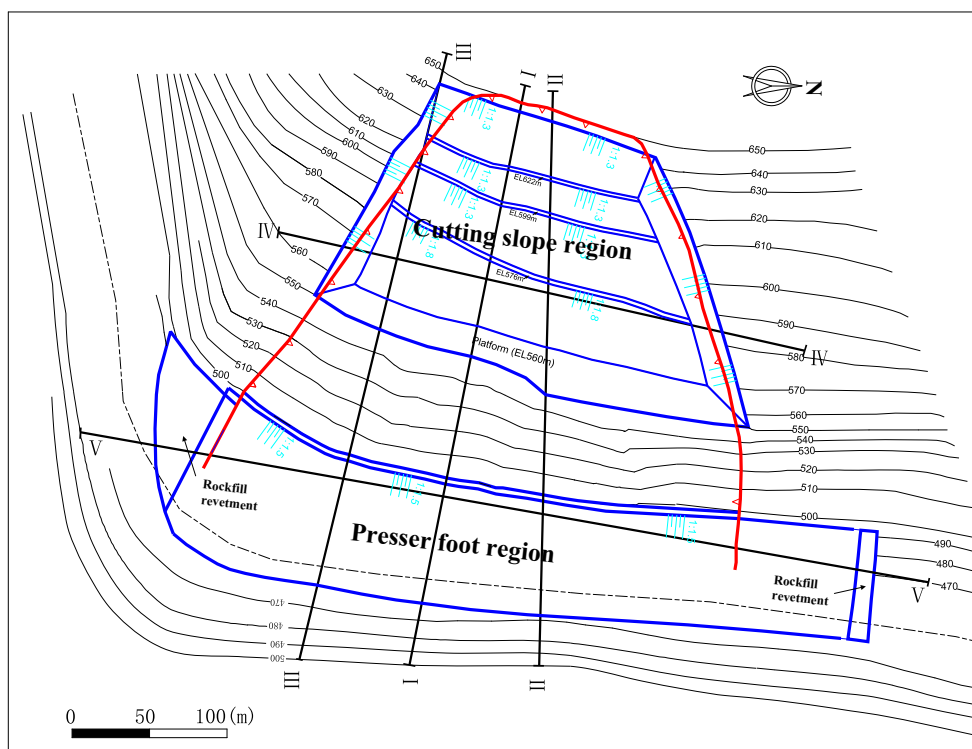
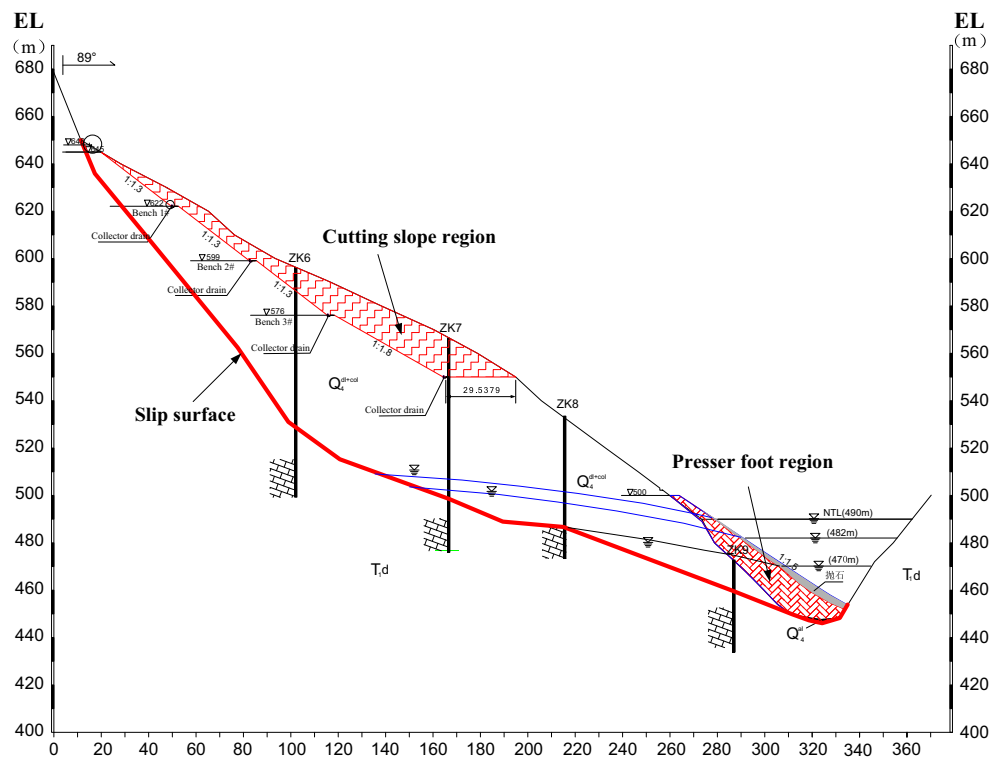


Fig. 9 Layout plan of the cutting and backfilling project

Fig. 10 The II–II geological profile displaying the cutting slope and presser foot regions



investment will be relatively small and the construction much simpler. Therefore, reinforcement measures including both cutting slope and backfill are taken to increase the stability of the Muchanghe landslide. Meanwhile, surface drainage works were also undertaken as a supplementary measure.

The layout plan for these works is shown in Fig. 9, with a cross section shown in Fig. 10. As for the excavation, three benches of 3 m width are set at elevations of 576, 599, and 622 m, respectively. The elevations of the top and bottom boundaries of the excavation area are 645 m and 560 m, respectively. A platform with a width ranging from 17 to 30 m is set at an elevation of 560 m. The gradient of the excavated slope is designed to be 1:1.3 or 1:1.8 to ensure its stability, and a rolling process for the slope surface after excavation was recommended. As for the backfilling project, it was designed so as to fill soil in a natural slope angle (about 33°) from the river bed of the Muchang River (at an elevation of 454 m) to an elevation of 500 m. A platform with a width of 4 m at an elevation of 500 m was built. After the completion of soil backfilling, riprap was used to cover and compress the backfilled soil within the elevations of 454 to 475 m. Moreover, to prevent the washout of the Muchang River, both sides of the backfilling area are filled with rock blocks.

As for the surface drainage project, there are six rows of transverse intercepting ditches and three lines of longitudinal drainage ditches set on the Muchanghe landslide

mass, as shown in Fig. 11. The first intercepting ditch (JA1), located at the trailing edge of the landslide mass, is mainly used to intercept surface water at the rear of the landslide. According to the design of the cutting and backfilling works, there are three benches and a platform at an elevation of 550 m, all of which are required to build intercepting ditches (JB2–JB5) at the inner side to hold up the accumulated water from the slope surface. The sixth row of intercepting ditches (JA6) is set at an elevation of about 500 m, which is located at the trailing edge of the backfilling area. Three longitudinal drainage ditches (P1–P3) are arranged so as to be situated at two sides, and in the middle, of the landslide mass.

Stability after treatment

The stability of the Muchanghe landslide after the execution of these works was evaluated by program JSlope3D. The mechanical parameters for the backfill material are also listed in Table 3. Figure 12 shows the division mesh and 3-D visualization model of the landslide mass after stabilization treatment. The size of columns used in the discretization of the landslide mass is the same as that used in Fig. 8. For comparison, the calculated factors of safety for the Muchanghe landslide after treatment are also listed in Table 4.

The results from Table 4 show that the reinforcement measures of cutting slope and backfill increased the safety

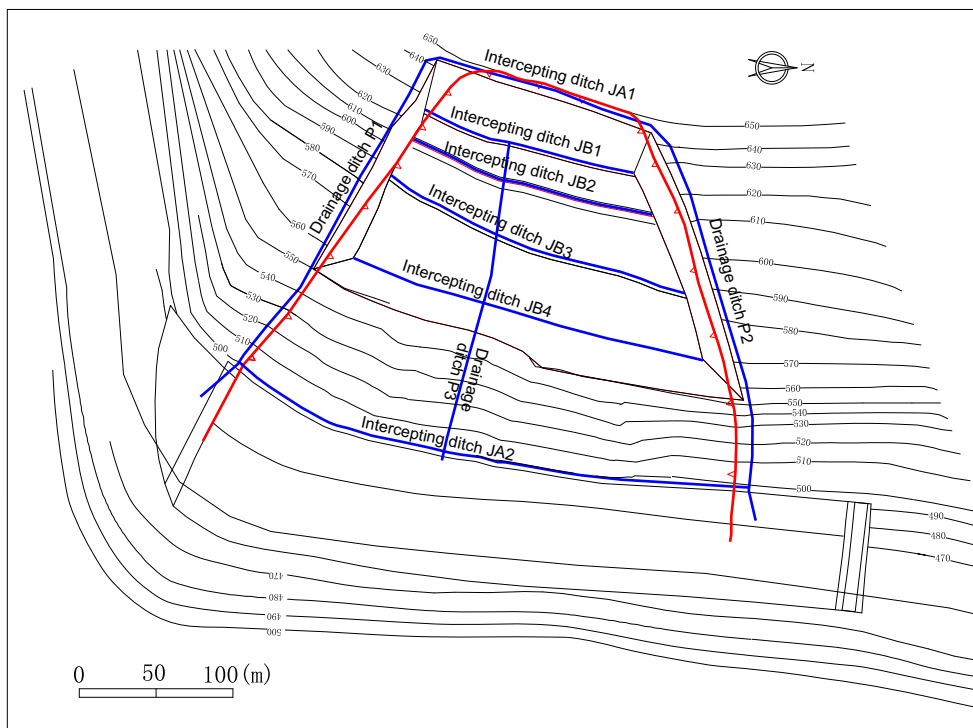


Fig. 11 Layout plan of the drainage project on the ground surface

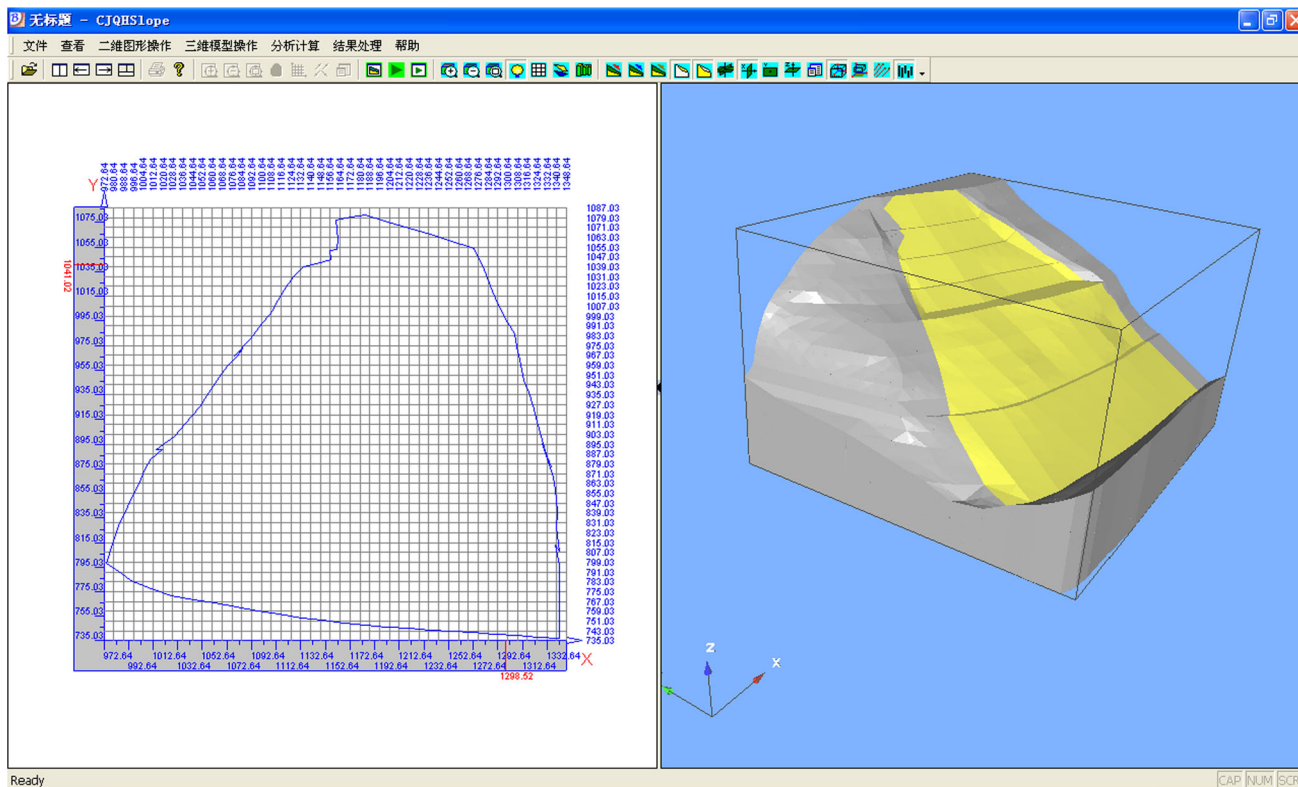


Fig. 12 3-D visualization model and the division mesh of the Muchanghe landslide after stabilization treatment

factor by 10–13 %. This demonstrates that cutting the slope back reduces the load acting on the trailing part of the landslide and backfilling increases the weight of the front part; therefore, the stability of the slope is improved due to a reduction in destabilizing force and an increase in the stabilizing resistance. At different impounded water levels, the Muchanghe landslide after reinforcement can meet the stability requirement of the design specification ($F > 1.05$). These results verify the reinforcement effect and feasibility of the measures taken.

After a six-month period, the construction of the stabilizing works at the Muchanghe landslide was fulfilled in April 2008. The routine observations of the deformation of the stabilized landslide indicate that the landslide is in a stable state during the reservoir operations.

Conclusions

Landslides induced by reservoir impounding have been frequently encountered during the operation of hydropower stations. The Muchanghe landslide began to deform in September 2006, when the water level in the Dongping reservoir reached an elevation of 470 m. With increasing impoundment, deformation increased and was mainly manifested by interconnected tensile fissures in its center. This study deals with the hazard assessment of the Muchanghe landslide after reservoir impounding and analyzes the reinforcement effect and feasibility of the stabilization measures. Through the use of this case study, the following conclusions can be drawn:

1. Considering that the sliding surface of the Muchanghe landslide has typical spatial features, we proposed a simplified 3-D limit equilibrium method for the stability assessment thereof: This is able to accommodate asymmetric slip surfaces. Using the proposed 3-D method, we can not only calculate the factor of safety, but also determine the direction of sliding of such landslides.
2. The proposed 3-D method was applied to the stability assessment of the Muchanghe landslide during reservoir impounding. The results showed that the landslide was in a stable state before reservoir impounding. After impounding, the factor of safety of the landslide gradually decreased with increasing water level, which would lead to that the stability of the landslide became worse. When the impounded water level reaches the normal pool level, the calculated factor of safety is < 1.0 and the landslide is unstable.
3. To prevent failure of the landslide, a reinforcement scheme involving the cutting back of the slope and backfilling was proposed to improve the stability of the

landslide. By using the proposed 3-D limit equilibrium method, the reinforcement scheme increased the safety factor by 10–13 %, which then meets the stability requirement of the landslide, at normal pool level, during the operation of the hydropower station.

Acknowledgments The work reported in this paper has received financial support from the National Natural Science Foundation of China (Nos. 51179137) and from National Basic Research Program of China (973 Program No. 2011CB013506). This support is gratefully acknowledged.

References

- Baker R, Leshchinsky D (1987) Stability analysis of conical heaps. *Soils Found* 27(4):99–110
- Chen RH, Chameau JL (1982) Three-dimensional limit equilibrium analysis of slopes. *Géotechnique* 33(1):31–40
- Chen ZY, Wang XG, Haberfield C (2001) A three-dimensional slope stability analysis method using the upper bound theorem part I: theory and methods. *Int J Rock Mech Min Sci* 38:369–378
- Chen ZY, Mi HL, Zhang FM, Wang XG (2003) A simplified method for 3D slope stability analysis. *Can Geotech J* 40:675–683
- Cheng YM, Yip CJ (2007) Three-dimensional asymmetrical slope stability analysis extension of Bishop's, Janbu's, and Morgenstern-Price's techniques. *J Geotech Geoenviron Eng* 133(12):1544–1555
- Corkum AG, Martin CD (2004) Analysis of a rock slide stabilized with a toe-berm: a case study in British Columbia, Canada. *Int J Rock Mech Min Sci* 41:1109–1121
- Fan YL, Zhao WB, Feng Y, Zhu NX (2007) Report on geology stability assessment of the Muchanghe landslide in Dongping reservoir (in Chinese). Hubei Provincial Water Resources and Hydropower Planning Survey and Design Institute, Wuhan
- Griffiths DV, Marquez RM (2007) Three-dimensional slope stability analysis by elasto-plastic finite elements. *Géotechnique* 57(6):537–546
- Huang CC, Tsai CC, Chen YH (2002) Generalized method for three-dimensional slope stability analysis. *J Geotech Geoenviron Eng* 128(10):836–848
- Hubei Provincial Water Resources and Hydropower Planning Survey and Design Institute 2007. Report on stabilization treatment design of the Muchanghe landslide in Dongping reservoir (in Chinese), Wuhan, China
- Hungr O, Salgado FM, Byrne PM (1989) Evaluation of a three-dimensional method of slope stability analysis. *Can Geotech J* 26:679–686
- Jiang QH, Chen YF, Zhou CB, Yeung MR (2013) Kinetic energy dissipation and convergence criterion of discontinuous deformations analysis (dda) for geotechnical engineering. *Rock Mech Rock Eng* 46(6):1443–1460
- Jin DL, Wang GF (1988) Tang Yanguang Landslide at the right bank of Zhexi Reservoir. In: Sun GZ (ed) *Typical landslides in China*. China Science Press, Beijing, pp 301–307
- Kiersch GA (1964) Vaiont reservoir disaster. *Civil Eng* 34:32–39
- Lam L, Fredlund DG (1993) A general limit equilibrium model for three-dimensional slope stability analysis. *Can Geotech J* 30:905–919
- Lee SG, Hencher SR (2013) Assessing the stability of a geologically complex slope where strong dykes locally act as reinforcement. *Rock Mech Rock Eng* 46(6):1339–1351
- Leshchinsky D, Huang CC (1992) Generalized three dimensional slope stability analysis. *J Geotech Eng* 118(11):1748–1764

- Stark TD, Eid HT (1998) Performance of three-dimensional slope stability methods in practice. *J Geotech Geoenviron Eng* 124(11):1049–1060
- Sun GH, Zheng H, Jiang W (2012) A global procedure for evaluating stability of three-dimensional slopes. *Nat Hazards* 61:1083–1098
- Ugai K (1989) A method of calculation of total factor of safety of slopes by elasto-plastic FEM. *Soils Found* 29(2):190–195
- Xu WJ, Jie YX, Li QB, Wang XB, Yu YZ (2014) Genesis, mechanism, and stability of the Dongmiaojia landslide, yellow river, China. *Int J Rock Mech Min Sci* 67:57–68
- Yamagami T, Jiang JC (1997) A search for the critical slip surface in three-dimensional slope stability analysis. *Soils Found* 37(3):1–16
- Zhang X (1988) Three-dimensional stability analysis of concave slopes in plan view. *J Geotech Eng* 114(6):658–671
- Zheng H (2012) A three-dimensional rigorous method for stability analysis of landslides. *Eng Geol* 145–146:30–40
- Zheng H, Liu DF, Li CG (2005) Slope stability analysis based on elasto-plastic finite element method. *Int J Numer Meth Eng* 64(14):1871–1888
- Zhou XP, Cheng H (2013) Analysis of stability of three-dimensional slopes using the rigorous limit equilibrium method. *Eng Geol* 160:21–33